

Study of dark matter physics in non-universal gaugino mass scenario

Junichiro Kawamura^{a*} and Yuji Omura^{b†}

^a*Department of Physics, Waseda University, Tokyo 169-8555, Japan*

^b*Kobayashi-Maskawa Institute for the Origin of Particles and the Universe (KMI),
Nagoya University, Nagoya 464-8602, Japan*

Abstract

We study dark matter physics in the Minimal Supersymmetric Standard Model with non-universal gaugino masses at the unification scale. In this scenario, the specific ratio of wino and gluino masses realizes the electro-weak scale naturally and achieves 125 GeV Higgs boson mass. Then, relatively light higgsino is predicted and the lightest neutral particle, that is dominantly given by the neutral component of higgsino, is a good dark matter candidate. The direct detection of the dark matter is sensitive to not only a higgsino mass but also gaugino masses significantly. The upcoming XENON1T experiment excludes the parameter region where bino or gluino is lighter than about 2.5 TeV if the higgsino and the gaugino mass parameters have same signs. We see that the direct detection of dark matter gives stronger bound than the direct search at the LHC experiment when higgsino sizably contributes to the dark matter abundance.

*E-mail address: junichiro-k@ruri.waseda.jp

†E-mail address: yujiomur@kmi.nagoya-u.ac.jp

Contents

1	Introduction	1
2	NUGM scenario	2
2.1	Review of NUGM	2
2.2	Mass spectrum of NUGM	3
2.3	LHC bounds	4
3	Dark matter physics	5
3.1	Neutralino sector	5
3.2	Thermal relic abundance	6
3.3	direct detection	7
3.4	Indirect detection	10
4	Numerical results	11
5	Conclusion	15

1 Introduction

Supersymmetry (SUSY) is a promising candidate for physics beyond the Standard Model (SM). The supersymmetric extension predicts the superpartners of the SM particles, and the masses of the SUSY particles are expected to be at least TeV-scale, in order to explain the origin of the electroweak (EW) scale.¹ In the Minimal Supersymmetric Standard Model (MSSM), there is a supersymmetric mass parameter, what is called μ -parameter, for higgsino that is the superpartner of Higgs bosons. In order to realize the EW scale without fine-tuning, μ -parameter should be EW-scale. Besides, the lightest particle in the MSSM becomes stable because of R-parity, so that higgsino becomes a good dark matter (DM) candidate if there is no lighter SUSY particle. So far, a lot of efforts are devoted to the SUSY search in the collider experiments and the dark matter observations [3]. There are no decisive signals of the SUSY particles, but higgsino is still one of the possible and attractive DM candidates that reveal the origin of the EW scale.

In the MSSM, there are a lot of parameters, so that we can consider many possibilities of the mass spectrum for the SUSY particles. The direct searches for the SUSY particles as well as the 125 GeV Higgs boson mass measurement at the LHC [4], however, constrain the parameter space strictly. It is getting very difficult to construct SUSY models, as long as the explanation of the EW scale is not discarded. One possible setup to achieve both the 125 GeV Higgs boson mass and the explanation of the EW scale is known as the Non-Universal Gaugino Masses (NUGM) scenario [5,6]. In this scenario, a suitable ratio of the wino mass to the gluino mass achieves the EW scale and the 125 GeV Higgs boson mass. Then, the μ -parameter is predicted to be close to the EW scale. The current status and the future prospect of the discovery of the SUSY particles at the LHC have been investigated in this scenario [7–9]. We find that the superpartners of top quark and gluon, what are called top squark and gluino, are promising particles to test this scenario. Expected reaches of these SUSY particles decaying to higgsinos are studied in Refs. [10,11].

Note that there are some models that lead such a ratio of the gauginos. One possibility is the mirage mediation [12–14], that is a mixture of the moduli mediation [15,16] and anomaly mediation [17,18]. The phenomenology of the mirage mediation is discussed before the Higgs boson discovery in Refs. [19–29] and after that in Refs. [30–36]. There are some works to realize the ratio of the gauginos in the GUT models [37] and superstring models [38].

In this kind of SUSY models, higgsino is light because of the explanation of the origin of the EW scale, and the SUSY particle is expected to be discovered in experiments. There are neutral and charged components in higgsino, and the neutral component mixes with bino and wino, and the charged component mixes with wino.² In our scenario, the gauginos are relatively heavy, so that all components of higgsino are light and almost degenerate; in fact, the mass difference is a few GeV [7,8]. Then, higgsino is hard to be detected at the LHC due to the certainly small mass differences. On the other hand, dark matter direct detection experiments

¹See for reviews e.g. [1,2].

²Wino and bino are the superpartners of $SU(2)_L$ and $U(1)_Y$ gauge bosons, respectively.

can efficiently observe higgsinos, if the neutral component of higgsino slightly mixes with the gauginos and dominates over our universe. It is also interesting that the higgsino mass should be lighter than about 1 TeV, if higgsino is thermally produced. Then, our DM mass, that mainly comes from the neutral component of higgsino, is predicted to be between the EW scale and 1 TeV.

In this paper, we study dark matter physics in the NUGM scenario. Direct detection experiments are sensitive to not only the higgsino mass itself, but also the gaugino masses, because the higgsino-gaugino mixing gives the most significant contribution to the detection rate. We also discuss the constraints from the LHC experiments, based on the results in Refs. [7–9]. We explicitly show the exclusion limit and the future prospect on the plane of the higgsino and the gaugino masses. In the end, we find that this scenario can be fully covered by the future experiments, as far as the gluino mass is below 2.5 TeV in a certain parameter set.

This paper is organized as follows. The NUGM scenario is reviewed in Section 2, and we discuss dark matter physics in Section 3. The results of numerical calculations are shown in Section 4. Section 5 is devoted to conclusion.

2 NUGM scenario

2.1 Review of NUGM

The NUGM scenario is known as one of the attractive SUSY models to realize μ -parameter near the EW scale and the 125 GeV Higgs boson mass simultaneously. The μ -parameter is related to the EW symmetry breaking scale through the minimization condition for the Higgs potential as

$$m_Z^2 \simeq 2|m_{H_u}^2| - 2|\mu|^2, \quad (1)$$

where m_Z is the Z-boson mass and $m_{H_u}^2$ is the soft scalar mass squared for the up-type Higgs boson. This relation shows that $|\mu|^2$ and $|m_{H_u}^2|$ should be around the EW scale to avoid the fine-tuning between those parameters. The μ -parameter is an unique SUSY-preserving parameter in the MSSM. On the other hand, all other dimensional parameters softly break SUSY and would be originated from some mediation mechanisms of SUSY breaking: i.e., the soft SUSY breaking terms would have same origin. Let us assume that the all ratios of soft SUSY breaking parameters are fixed by some mediation mechanisms and the overall scale is given by M_0 . In this assumption, Eq. (1) corresponds to the relation between μ and M_0 . In Ref. [39], the parameter, Δ_x , to measure the sensitivity of the parameter x to the EW scale is introduced:

$$\Delta_x = \left| \frac{\partial \ln m_Z^2}{\partial \ln x^2} \right| (x = \mu, M_0). \quad (2)$$

Since $m_{H_u}^2(m_{\text{SUSY}})$ is expressed as a quadratic polynomial function of the boundary conditions, we can derive $\Delta_\mu + \Delta_{M_0} = 1$ at the tree-level and $\Delta_\mu \simeq \Delta_{M_0}$ is satisfied. Thus the tuning

of the μ -parameter represents the degree of tuning to realize the EW symmetry breaking in the model. From the relation Eq. (1), the tuning measure of the μ -parameter can be written as $\Delta_\mu = 2|\mu|^2/m_Z^2$ up to radiative corrections to the condition, so that small $|\mu|$ is simply required to avoid the fine-tuning in this assumption. The details of this kind of discussions in the NUGM scenario are shown in Refs. [9, 40]. We proceed to study collider and dark matter phenomenology with the NUGM in this assumption.

In this paper, we assume universal soft scalar mass m_0 and A-term A_0 , while the gaugino masses $M_{1,2,3}$ are non-universal at the gauge coupling unification scale ($\simeq 10^{16}$ GeV). We assume the ratio of two Higgs vacuum expectation values (VEVs) $\tan\beta \equiv \langle H_u \rangle / \langle H_d \rangle = 10$ throughout this paper. The soft mass squared $m_{H_u}^2$ at $m_{\text{SUSY}} = 1$ TeV relates to the boundary conditions at the unification scale as

$$m_{H_u}^2(m_{\text{SUSY}}) \simeq 0.005M_1^2 - 0.005M_1M_2 + 0.201M_2^2 - 0.021M_1M_3 - 0.135M_2M_3 - 1.57M_3^2 + A_0(0.011M_1 + 0.065M_2 + 0.243M_3 - 0.099A_0) - 0.075m_0^2. \quad (3)$$

This relation shows that the contribution from the gluino mass is dominant among the renormalization group (RG) effects, but we find that the gluino mass contribution can be canceled by the RG effects from the other gaugino masses $M_{1,2}$. In particular, the M_2^2 term cancels the M_3^2 term if the ratio of M_2/M_3 satisfies $M_2/M_3 \simeq 3$ -4. Similarly, the top squark mass parameters $m_{\tilde{t}_L}^2$, $m_{\tilde{t}_R}^2$ and A_t at $m_{\text{SUSY}} = 1$ TeV are related to the boundary conditions as

$$m_{\tilde{t}_L}^2(m_{\text{SUSY}}) \simeq -0.007M_1^2 - 0.002M_1M_2 + 0.354M_2^2 - 0.007M_1M_3 - 0.051M_2M_3 + 3.25M_3^2 + (0.004M_1 + 0.025M_2 + 0.094M_3 - 0.039A_0)A_0 + 0.622m_0^2, \quad (4)$$

$$m_{\tilde{t}_R}^2(m_{\text{SUSY}}) \simeq 0.044M_1^2 - 0.003M_1M_2 - 0.158M_2^2 - 0.014M_1M_3 - 0.090M_2M_3 + 2.76M_3^2 + (0.008M_1 + 0.044M_2 + 0.162M_3 - 0.066A_0)A_0 + 0.283m_0^2, \quad (5)$$

$$A_t(m_{\text{SUSY}}) \simeq -0.032M_1 - 0.237M_2 - 1.42M_3 + 0.277A_0. \quad (6)$$

We see that $A_t(m_{\text{SUSY}})$ increases and $m_{\tilde{t}_R}^2(m_{\text{SUSY}})$ decreases as the wino mass M_2 increases. Note that the latter effect is induced by the top Yukawa coupling. As a result, the ratio $A_t^2/\sqrt{m_{\tilde{t}_L}^2 m_{\tilde{t}_R}^2}$ increases and the SM-like Higgs boson mass around 125 GeV can be achieved due to the relatively large wino.

2.2 Mass spectrum of NUGM

We see that the suitable wino-to-gluino mass ratio reduces the μ -parameter and also enhances the Higgs boson mass. Besides, some of sparticle masses are within reaches of the LHC experiment thanks to the sizable left-right mixing of the top squarks [7, 8].

When the wino mass is large, left-handed sparticles become heavy due to the RG evolution. The right-handed slepton masses are determined by the bino mass, while the right-handed squark masses mainly depend on both the gluino and bino masses. The bino mass plays a

crucial role in shifting the top squark mass, as well. This means that the bino mass have to be so heavy that the top squark mass is enough heavy to be consistent with the LHC results.

Another important point derived from the relatively heavy bino and wino is that the mass differences among the components of higgsino become small. The mass differences are induced by the mixing with higgsino and gauginos, so that these are suppressed by the bino and wino masses as explicitly shown in next section. The mass differences among the components of higgsino are typically 2 GeV as shown in Ref. [7]. This small mass difference makes it difficult to detect higgsino directly at the LHC, because their daughter particles are too soft to be distinguished from backgrounds and their lifetimes are too short to be recognized as charged tracks unlike the case that wino is the lightest SUSY particle (LSP) [41]³. This feature also indicates that we can treat all of the particles from higgsino as invisible particles at the LHC.

Let us summarize the important features of our mass spectrum discussed below:

- All gauginos are $\mathcal{O}(1)$ TeV.
- The higgsino mass is between the EW scale and 1 TeV, and the mass differences are $\mathcal{O}(1)$ GeV.
- Right-handed top squark is relatively light.

2.3 LHC bounds

In our scenario, the top squark and the gluino are the good candidates to be detected at the LHC. The current exclusion limit and the future prospect have been studied in Refs. [7–9].

In the NUGM scenario, a top squark decays as $\tilde{t}_1 \rightarrow t\tilde{\chi}_{1,2}^0/b\tilde{\chi}_1^\pm$ where each branching fraction is 50% as long as the mass difference between the top squark and each of the higgsino-like particles is significantly larger than the top quark mass. Note that the neutralinos consist of higgsino that slightly mixes with wino and bino in our scenario. The relevant top squark searches at the LHC are discussed in Ref. [44] and Ref. [45]. The former analysis aims to a pair of bottom squarks that decay as $\tilde{b}_1\tilde{b}_1 \rightarrow b\tilde{\chi}^0b\tilde{\chi}^0$. This gives same signal as $\tilde{t}_1\tilde{t}_1 \rightarrow b\tilde{\chi}^\pm b\tilde{\chi}^\pm$ in the NUGM scenario. The latter analysis aims to hadronically decaying top squarks, $\tilde{t}_1\tilde{t}_1 \rightarrow t\tilde{\chi}^0t\tilde{\chi}^0 \rightarrow bj\tilde{\chi}^0bj\tilde{\chi}^0$. In Ref. [45], the signal regions require more than 4 jets, where 2 of these should be b-tagged. Such signal regions will be sensitive to events $\tilde{t}_1\tilde{t}_1 \rightarrow t(\rightarrow bj\tilde{\chi}^0)\tilde{\chi}^0b\tilde{\chi}^\pm$ in the NUGM scenario, although this analysis is not completely optimized. This decay pattern is realized in almost half of the events with the pair produced top squarks if the mass difference between the top squark and higgsino is enough large. Thus this channel that targets to the hadronically decaying top squark is sensitive to the large mass difference region, while the former channel that targets to bottom squarks decaying to a bottom quark and a neutralino is sensitive to the mass degenerate region. Referring the analysis in Ref. [9], top squark lighter than 800 GeV is excluded if $\mu \lesssim 200$ GeV is satisfied, and top squark lighter than 600 GeV is excluded in the

³There are recent works to study searching for charged higgsinos that exploit their relatively long lifetime [42, 43].

range with $200 \text{ GeV} \lesssim \mu \lesssim 270 \text{ GeV}$. There is no exclusion limit for top squarks if μ is greater than 270 GeV.

In present scenario, a gluino decays as $\tilde{g} \rightarrow t\tilde{t}_1 \rightarrow t + t\tilde{\chi}^0/b\tilde{\chi}^\pm$. Hence, the the signal from the gluino pair production is expected to have 4 b-tagged jets, jets/leptons coming from 2-4 W-bosons and large missing energies in the final state. The analysis in Ref. [46] aims to this type of signals, and we refer the exclusion limit obtained in Ref. [9]. Gluino lighter than 1.8 TeV is excluded if the μ -parameter is less than 800 GeV. The bound is relaxed if the mass difference is smaller than about 300 GeV.

Note that there is another channel, $\tilde{g} \rightarrow g\tilde{\chi}^0$, that is induced by the top squark loop. If the mass difference between gluino and higgsino is near or less than the top quark mass, this decay channel becomes important. We need to consider the limits based on data such as Ref. [47], but it is beyond the scope of this paper.

Let us comment on the case with light bino. If gluino is enough heavy, bino can be as light as higgsino and top squark can also decay to bino. The decay is, however, usually suppressed unless bino is significantly lighter than higgsino because the coupling of bino with top squark is much weaker than the one of higgsinos because of the top Yukawa coupling. Such a light bino is less attractive from the experimental point of view. If the bino mass is light, gluino has to be much heavier than the experimental reach in order to shift the top squark mass. Then, the light bino case would be unfavorable from the naturalness point of view. Furthermore, it is known that bino LSP tends to overclose the universe and some dilution mechanisms are necessary.

3 Dark matter physics

3.1 Neutralino sector

In our study, we assume that the signs of all the gaugino masses are positive and the sign of the μ -parameter is either negative or positive. After the EW symmetry breaking, gauginos and higgsino are mixed each other. The neutralino mass matrix in a basis of $\psi = (\tilde{B}, \tilde{W}, \tilde{H}_d^0, \tilde{H}_u^0)$ is given by

$$M_{\tilde{\chi}} = \begin{pmatrix} M_1 & 0 & -c_\beta s_W m_Z & s_\beta s_W m_Z \\ 0 & M_2 & c_\beta c_W m_Z & -s_\beta c_W m_Z \\ -c_\beta s_W m_Z & c_\beta c_W m_Z & 0 & -\mu \\ s_\beta s_W m_Z & -s_\beta c_W m_Z & -\mu & 0 \end{pmatrix}, \quad (7)$$

where $c_\beta = \cos \beta$, $s_\beta = \sin \beta$, $c_W = \cos \theta_W$ and $s_W = \sin \theta_W$ are defined and θ_W is the Weinberg angle. This matrix is diagonalized by a unitary matrix N as

$$\psi_i = N_{ij} \tilde{\chi}_j \quad \text{and} \quad N^\dagger M_{\tilde{\chi}} N = \text{diag}(m_{\tilde{\chi}_1}, m_{\tilde{\chi}_2}, m_{\tilde{\chi}_3}, m_{\tilde{\chi}_4}). \quad (8)$$

The masses, $m_{\tilde{\chi}_1}$, $m_{\tilde{\chi}_2}$, $m_{\tilde{\chi}_3}$ and $m_{\tilde{\chi}_4}$ approach to M_1 , M_2 , μ , and $-\mu$ in the limit that m_Z is vanishing, respectively. The mass eigenstate $\tilde{\chi}_3$ ($\tilde{\chi}_4$) becomes the lightest one if the μ -parameter is positive (negative) and $|\mu| < M_1, M_2$.

The neutralino-neutralino-Higgs coupling, $\mathcal{L} \ni (1/2)\lambda_{hnn}h\bar{\chi}_n\tilde{\chi}_n$, is given by

$$\lambda_{hnn} = g(s_\alpha N_{3n} + c_\alpha N_{4n})(N_{2n} - t_W N_{1n}), \quad (9)$$

where t_W , s_α and c_α are short for $\tan\theta_W$, $\sin\alpha$ and $\cos\alpha$, respectively. α is a mixing angle of the Higgs boson. The mixing matrix is given by

$$(N_{11}, N_{21}, N_{31}, N_{41}) = \left(1, 0, -\frac{m_Z s_W (c_\beta M_1 + s_\beta \mu)}{M_1^2 - \mu^2}, \frac{m_Z s_W (c_\beta \mu + s_\beta M_1)}{M_1^2 - \mu^2}\right), \quad (10)$$

$$(N_{12}, N_{22}, N_{32}, N_{42}) = \left(0, 1, \frac{m_Z c_W (c_\beta M_2 + s_\beta \mu)}{M_2^2 - \mu^2}, -\frac{m_Z c_W (c_\beta \mu + s_\beta M_2)}{M_2^2 - \mu^2}\right), \quad (11)$$

$$(N_{13}, N_{23}, N_{33}, N_{43}) = \frac{1}{\sqrt{2}} \left(\frac{m_Z s_W (c_\beta + s_\beta)}{M_1 - \mu}, -\frac{m_Z c_W (c_\beta + s_\beta)}{M_2 - \mu}, 1, -1\right), \quad (12)$$

$$(N_{14}, N_{24}, N_{34}, N_{44}) = \frac{1}{\sqrt{2}} \left(\frac{m_Z s_W (c_\beta - s_\beta)}{M_1 + \mu}, -\frac{m_Z c_W (c_\beta - s_\beta)}{M_2 + \mu}, 1, 1\right), \quad (13)$$

where $m_Z \ll |M_{1,2} \pm \mu|$ is assumed.

3.2 Thermal relic abundance

It is known that the thermal relic density of the purely higgsino LSP saturates the universe when the higgsino mass is about 1 TeV [48, 49]. If we assume that there is no dilution effect after the thermal production of the LSP, the higgsino-like LSP heavier than 1 TeV overcloses the universe and is cosmologically excluded unless the higgsino and another sparticle, such as a top squark, are so degenerate that co-annihilation processes between them reduce the relic density.

Let us comment on possibilities that gauginos contribute to dark matter considerably. In our scenario, the wino mass should be as large as the gluino mass at the TeV scale and it hardly contributes to the dark matter. The bino mass can be as light as the higgsino mass if the gluino mass is enough large to keep the top squark mass. It was interesting that the well-tempered bino-higgsino LSP explains the observed abundance in the thermal scenario [50], but most of parameter space has been already excluded by the direct detections as will be discussed later ⁴.

In our scenario, the relic DM abundance thermally produced may not be sufficient to satisfy the observed DM abundance in our universe. When we denote the relic abundance of the LSP as $\Omega_\chi h^2$, we can simply consider two possibilities to saturate the observed value, $\Omega_{\text{obs}} h^2 = 0.1188 \pm 0.0001$ [52]:

- (A) $\Omega_\chi h^2$ is only given by the thermal production, and $\Omega_\chi h^2 \leq \Omega_{\text{obs}} h^2$ is satisfied.
- (B) $\Omega_\chi h^2 = \Omega_{\text{obs}} h^2$ is always satisfied, assuming non-thermal production of LSP works.

⁴ There are narrow regions where the thermal bino-higgsino LSP explains the abundance by the Higgs- or Z-boson resonances without tension with the DM direct detection experiments [51].

In the case (A), what is called *thermal scenario*, the LSP may not saturate our universe, depending on the parameter region. Then, we need other dark matter candidates such as axion to achieve the observed relic abundance of DM.

In the case (B), what is called *non-thermal scenario*, we simply assume that the LSP dominates our universe and satisfies $\Omega_\chi h^2 = \Omega_{\text{obs}} h^2$. We do not explicitly calculate the relic abundance, but several mechanisms for the non-thermal productions have been proposed so far. For instance, it is known that the decays of long-lived heavy particles, such as gravitino, saxion and moduli field, can significantly produce the LSP after the LSP is frozen out from the thermal bath [53–56].

Note that the important difference of the two scenarios is whether $\Omega_\chi h^2 < \Omega_{\text{obs}} h^2$ is allowed or not. In our study, we estimate the thermal relic density of the LSP, and we exclude the region with $\Omega_\chi h^2 > \Omega_{\text{obs}} h^2$ ⁵. When we estimate the direct detection rate of DM, the abundance of the LSP is important. Then we draw the exclusion limits of both cases.

3.3 direct detection

The direct detection for dark matter is a promising way to probe the neutralino sector of the MSSM. The current limits on the spin-independent and spin-dependent cross sections are given by the XENON100 [57–59], LUX [60, 61], PANDAX-II [62, 63] and PICO [64, 65]. The XENON1T [66] and LZ [67] will cover wider range in near future.

Let us discuss spin-independent cross section of neutralino scattering with nucleons. Note that the limits on the gaugino masses from the spin-independent cross section are stronger than those from the spin-dependent cross section in most cases.

At tree-level, spin-independent scatterings are induced by the t-channel Higgs boson exchange and the s-channel squark exchange. Since only one top squark is light in the NUGM scenario, the latter contribution is negligibly small. The mixing between gauginos and higgsino are important in the Higgs boson exchange, because the LSP-LSP-Higgs coupling in the mass eigenstate basis is originated from the gaugino-higgsino-Higgs couplings in the gauge eigenstate basis. In the limit of $m_Z \ll |M_{1,2} \pm \mu|$, the mixing effects are suppressed by $m_Z/|M_{1,2} \pm \mu|$ as shown in Eqs. (12) and (13).

It has been shown that there is a parameter set to lead vanishing gaugino-higgsino mixing, what is called the blind spot [68]. As we see Eqs.(9), (10) and (11), the mixing is proportional to $M_{1,2} + \mu \sin 2\beta$, so that the mixing vanishes when the relative signs of $M_{1,2}$ and μ are opposite, and $|M_{1,2}| \lesssim |\mu|$ and $\tan \beta \gtrsim 1$ are satisfied. Thus the blind spot appears only in the gaugino-like LSP scenario.

Note that the mixing is suppressed when the LSP is higgsino-like and signs of μ and $M_{1,2}$ are opposite, as we can see from Eqs.(12) and (13). Since the mixing is proportional to $1 \pm \sin 2\beta$, smaller $\tan \beta$ induces larger enhancement (suppression) for the same (opposite) sign. We need $\tan \beta \gtrsim 10$ in order to realize the SM-like Higgs boson mass unless the sparticle masses are

⁵ Note that this region is not truly excluded in the non-thermal scenario, but such region satisfies $|\mu| \gtrsim 1.0$ TeV that is less attractive from both the testability and the naturalness point of view.

much heavier than 1 TeV, so that such effect is at most 20%-level. Thus we conclude that the gaugino-higgsino mixing is sizable and the factor, $1 \pm \sin 2\beta$, leads significant difference between the positive and the negative μ -parameter cases in the DM scattering cross section.

The spin-independent cross section per nucleon at the tree-level can be written as

$$\sigma_N^{\text{SI}} = \frac{g^2}{4\pi} \frac{m_N^4}{m_h^4 m_W^2} \left(1 + \frac{m_N}{m_\chi}\right)^{-2} \left[\frac{2}{9} + \frac{7}{9} \sum_{q=u,d,s} f_{T_q}^N \right]^2 \lambda_{h\chi\chi}^2, \quad (14)$$

where m_N is the nucleon mass and $m_N f_{T_q}^N = \langle N | m_q \bar{q}q | N \rangle$. In the decoupling limit $m_A \gg m_Z$ that is a good approximation for our case, using Eqs. (12) and (13), the LSP-LSP-Higgs coupling $\lambda_{h\chi\chi}$ is derived from Eq. (9):

$$\lambda_{h\chi\chi} = \frac{g}{2} (1 \pm s_{2\beta}) c_W \left(\frac{m_Z}{M_2 - |\mu|} + t_W^2 \frac{m_Z}{M_1 - |\mu|} \right), \quad (15)$$

where \pm corresponds to a sign of the μ -parameter.

We list the explicit values of masses and observables at the sample points in Table 1. We can see that the A-term is same order as other input parameters, but the Higgs boson mass is about 125 GeV owing to the suitable wino-to-gluino mass ratio. The top squark mass is about 1.5 TeV and the gluino mass is 2-3 TeV, so that they could be in the reach of the HL-LHC. The bino and wino masses are between 2 TeV and 5 TeV and they are far beyond the experimental reach of the LHC experiment.

When $|\mu| = 250(1000)$ GeV in the samples (a), (b), (c) and (d), the thermal relic abundance is $\sim 0.01(0.1)$. The self-annihilation rate of the neutralinos in the zero-velocity limit, denoted by $\langle \sigma v \rangle_0$, is $\mathcal{O}(0.1 - 1.0) \times 10^{-25} [\text{cm}^3/\text{s}]$ and they are dominantly decaying to weak gauge bosons. These processes are induced by the t-channel neutralino or chargino exchange, and then the rate is determined by the higgsino mass itself. These are important for the indirect detections as discussed below.

We also show the spin-dependent and spin-independent LSP-proton cross sections, σ_{SD} , σ_{SI} , calculated by using micrOMEGA-4.2.5 [69]. σ_{SI}^h is obtained from Eqs. (14) and (15), where $f_{T_q}^p$ are taken same as the values adopted in micrOMEGA [70]. We can see the SI cross section is well described by the tree-level Higgs-exchanging process, but there are small deviations from the results of micrOMEGA.

A dominant source for the deviation come from the QCD corrections to the heavy quark matrix elements [71], which enhance the cross section about 10% against the tree-level contribution. Besides, the top squarks could give contribution to the cross section, when a mass difference $m_{\tilde{t}_1}^2 - m_\chi^2$ is small. However, it is known that the leading contribution, which is suppressed by $(m_{\tilde{t}_1}^2 - m_\chi^2) m_t^2$, is proportional to the size of non-trivial mixing of the top squarks [72]. The top squark is almost right-handed in our scenario and thus such contribution can not be sizable. We take the top squark corrections derived in Ref. [72] into account, and confirm that these are about 1% against the tree-level contribution at the sample (d) and fewer for the

Table 1: Values of boundary conditions at the unification scale M_U , Higgs boson masses, sparticle masses and dark matter observables at several sample points.

input [GeV]	(a)	(b)	(c)	(d)
μ	-250	250	-1000	1000
$M_1(M_U)$	10000	10000	5000	5000
$M_3(M_U)$	1000	1000	1500	1500
$m_0(M_U)$	1000	1000	1000	1000
output [GeV]				
$M_2(M_U)$	4223	4175	4698	4504
$A_0(M_U)$	-2378	-2325	-1916	-1657
mass [GeV]				
m_h	125.0	125.0	125.0	125.0
m_A	3349	3326	3351	3248
$m_{\tilde{t}_1}$	1606	1636	1431	1581
$m_{\tilde{t}_2}$	2780	2762	3582	3520
$m_{\tilde{g}}$	2250	2250	3225	3223
$m_{\tilde{\chi}_1^0}$	258.8	255.7	1016	1013
$m_{\tilde{\chi}_2^0}$	260.5	258.3	1019	1017
$m_{\tilde{\chi}_3^0}$	3438	3400	2239	2237
$m_{\tilde{\chi}_4^0}$	4455	4454	3839	3682
$m_{\tilde{\chi}_1^\pm}$	260.5	257.1	1018	1015
$m_{\tilde{\chi}_2^\pm}$	3439	3400	3840	3682
observables				
$\Omega_\chi h^2$	7.82×10^{-3}	7.58×10^{-3}	1.14×10^{-1}	1.16×10^{-1}
$\langle \sigma v \rangle_0 \times 10^{25} [\text{cm}^3/\text{s}]$	1.39	1.42	0.104	0.105
$\text{Br}(\chi\chi \rightarrow W^+W^-)$	0.533	0.535	0.488	0.489
$\text{Br}(\chi\chi \rightarrow ZZ)$	0.436	0.435	0.408	0.407
$\sigma_{\text{SD}} \times 10^{-6} [\text{pb}]$	1.096	1.138	0.1677	0.1757
$\sigma_{\text{SI}} \times 10^{-11} [\text{pb}]$	3.499	8.505	8.918	22.37
$\sigma_{\text{SI}}^h \times 10^{-11} [\text{pb}]$	3.302	7.793	7.853	19.50

other sample points. We have checked that our results agree with the results of micrOMEGAS exhibited in Table 1 within several %-level after including these effects. There are potentially sizable corrections from neutralino/Z-boson and chargino/W-boson mediated loop diagrams, where the neutralino and chargino are higgsino-like, but these are almost canceled out among them as shown in Ref. [73].

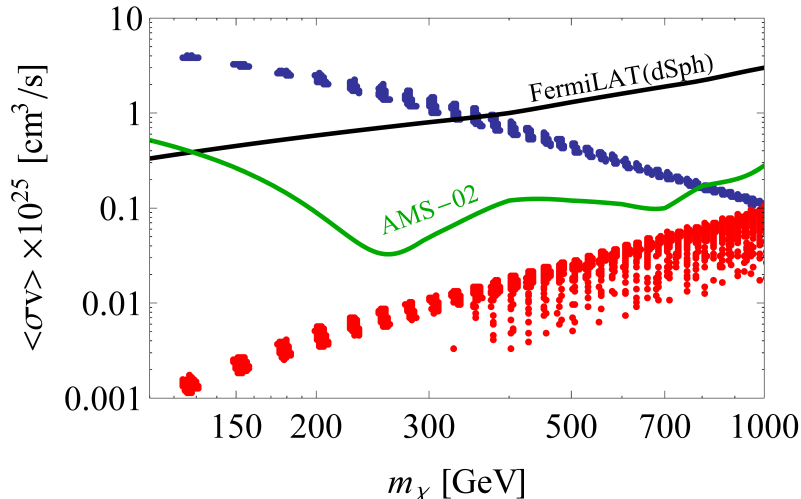


Figure 1: Exclusion limits and expected values in the NUGM scenario of the dark matter annihilation cross section. The blue (red) dots correspond to the non-thermal (thermal) scenario.

3.4 Indirect detection

Let us comment on indirect detections for the dark matter. A pair of neutralinos decay to W^+W^- or ZZ with the zero-velocity cross section: that is $\mathcal{O}(10^{-25})[\text{cm}^3/\text{s}]$ as shown in Table 1.

One of the most promising observables may be the neutrino flux from the sun. The capture rate of neutralino by the sun is determined by the interaction between neutralino and nucleons. Since the spin-dependent cross section is much larger than the spin-independent one, the observations would give significant bounds on the spin-dependent cross section. The weak bosons produced by the annihilation of dark matter decay to neutrinos. The observed limit of neutrinos given by the IceCube is 3.76×10^{-5} pb when the dark matter mass is 500 GeV and they decay to W-bosons exclusively [74]. This limit is comparable to the expected limit at the XENON1T [57]. We will see that exclusion limits for the parameter space from the XENON1T are much weaker than limits from the spin-independent cross section, so that the current limit from IceCube experiment can not be important one.

Cosmic ray observations such as photons, positrons and anti-protons could be powerful tools to detect dark matter. These limits of the annihilation cross section of DM reach to $\mathcal{O}(10^{-25})[\text{cm}^3/\text{s}]$ and the parameter region discussed in present paper is competing with these bounds. We consider the recent experimental results obtained by the Fermi-LAT [75] and AMS-02 [76]. The former observes gamma rays coming from the dwarf spheroidal satellite galaxies (dSphs) of the Milky Way and the latter observes anti-protons coming from dark matter annihilations in the Milky Way. We refer the exclusion limit from the AMS-02 experiment obtained in the analysis [77]⁶. The Fermi-LAT experiment also observes gamma-rays coming

⁶ Similar analysis is done in Ref. [78].

from the galactic center and this potentially gives significant constraints on the dark matter annihilation rate. However, the results are highly dependent on dark matter density profiles [79], so that we do not discuss about this in present paper.

Figure 1 shows the upper limits on the annihilation cross section from the recent results of the Fermi-LAT (black line) and the AMS-02 (green line). The dots are predictions from the NUGM scenario and obtained by the parameter scanning to draw figures in next section. We plot the points with $M_1 \geq 2.5$ TeV at the unification scale. The blue dots indicate the lightest neutralino mass and the annihilation rate itself, but it is multiplied by $(\Omega_\chi/\Omega_{\text{obs}})^2$ for the red dots. Since the higgsino-like dark matter dominantly annihilate to W-bosons or Z-bosons by the t-channel exchange of the higgsino-like chargino or neutralino, the annihilation rate is mostly determined by the higgsino mass itself and almost independent of other parameters. We see that the Fermi-LAT result excludes the neutralino lighter than about 300 GeV and the AMS-02 excludes the neutralino lighter than about 800 GeV in the non-thermal scenario. On the other hand, the indirect detections do not give limits on the thermal scenario, because the annihilation rate is suppressed by the factor $(\Omega_\chi/\Omega_{\text{obs}})^2$. Exclusion limits on the higgsino dark matter produced from some non-thermal processes at the Fermi-LAT and the future planned CTA experiments [80] have been discussed in Ref. [81].

4 Numerical results

Based on the above discussion, we summarize the experimental bounds and show the allowed region. As mentioned in Section 3.2, our analysis of the relic density includes two possibilities: thermal scenario and non-thermal scenario. We calculate only thermal relic density and exclude the region with $\Omega_\chi h^2 > \Omega_{\text{obs}} h^2$. The difference of two scenarios only appear in the bound from the direct detection of DM. $\Omega_\chi h^2 < \Omega_{\text{obs}} h^2$ is possible in the thermal scenario, so that the bound is relaxed.

Figure 2 shows the allowed region for the dark matter observables, the top squark mass and exclusion limits from the collider experiments. We assume $m_0 = 1$ TeV, $M_3 = 1.5$ TeV at the unification scale and A_0, M_2 are chosen to realize the SM-like Higgs boson mass and the μ -parameter at each point. We take the ratio of the Higgs VEVs as $\tan \beta = 10$. We use softsusy-3.5.1 [82] to calculate the RG effects and the mass spectrum of sparticles and Higgs bosons. Their width and branching ratios are calculated by SDECAY and HDECAY [83]. The dark matter observables are calculated by micrOmega-4.2.5 [69].

The red lines represent the thermal relic density of the neutralino, where the solid (dashed) lines correspond to $\Omega_\chi/\Omega_{\text{obs}} = 0.5$ (0.1) respectively. $\Omega_\chi = \Omega_{\text{obs}} = 0.1188 \pm 0.0001$ [52] is achieved in the red band around $|\mu| \simeq 1$ TeV. The thermal relic density of the dark matter exceeds the observed value, $\Omega_\chi > \Omega_{\text{obs}}$, in the light gray region, so that this region is excluded if there is no dilution effects after the freeze-out of the neutralino. The gray region at $|\mu| \leq 90$ GeV is excluded by the LEP experiment [84]. Although the charged and neutral components of higgsino are certainly degenerate, they can be probed by the mono-photon channel. The

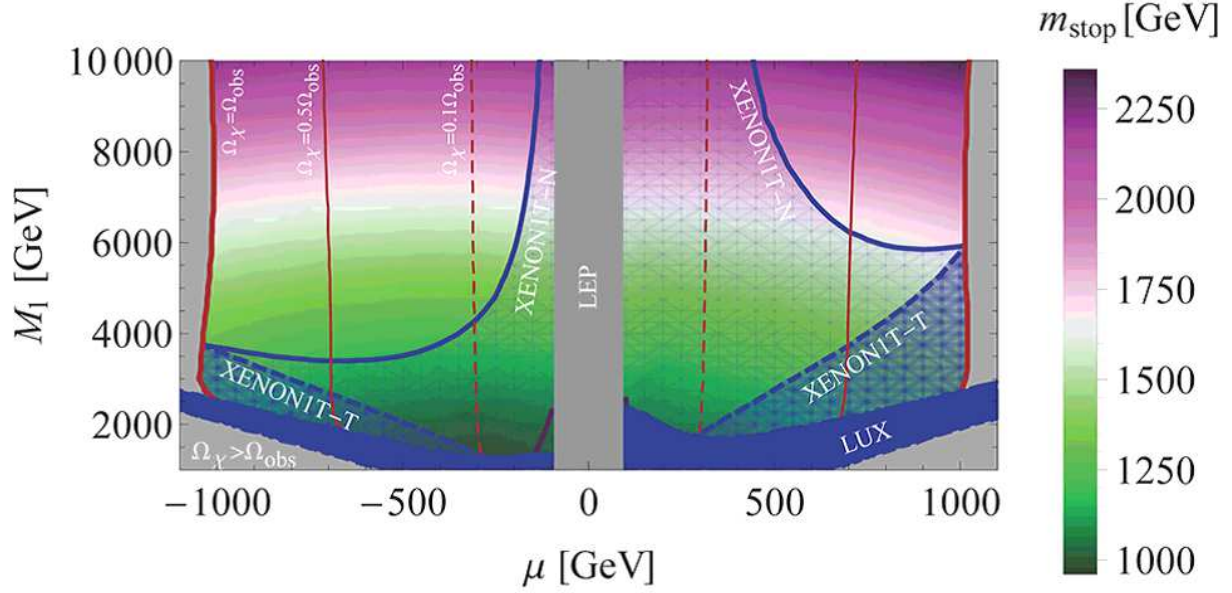


Figure 2: Values of the dark matter observables with $M_3 = 1.5$ TeV.

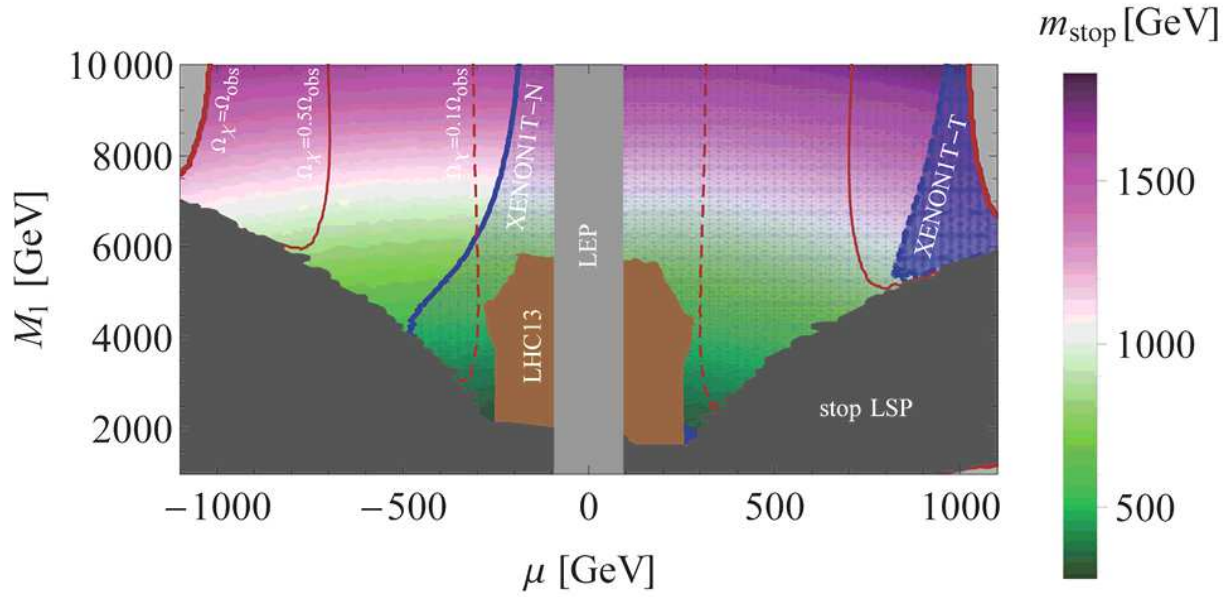


Figure 3: Values of the dark matter observables with $M_3 = 1.0$ TeV.

background color represent the mass of the lightest top squark. The purple line around $M_1 \lesssim 2.0$ TeV and $\mu \simeq -100$ GeV is the expected exclusion limits for the spin-dependent cross section from the XENON1T experiment [57].

The spin-independent cross section exceeds the current limit given by the LUX experi-

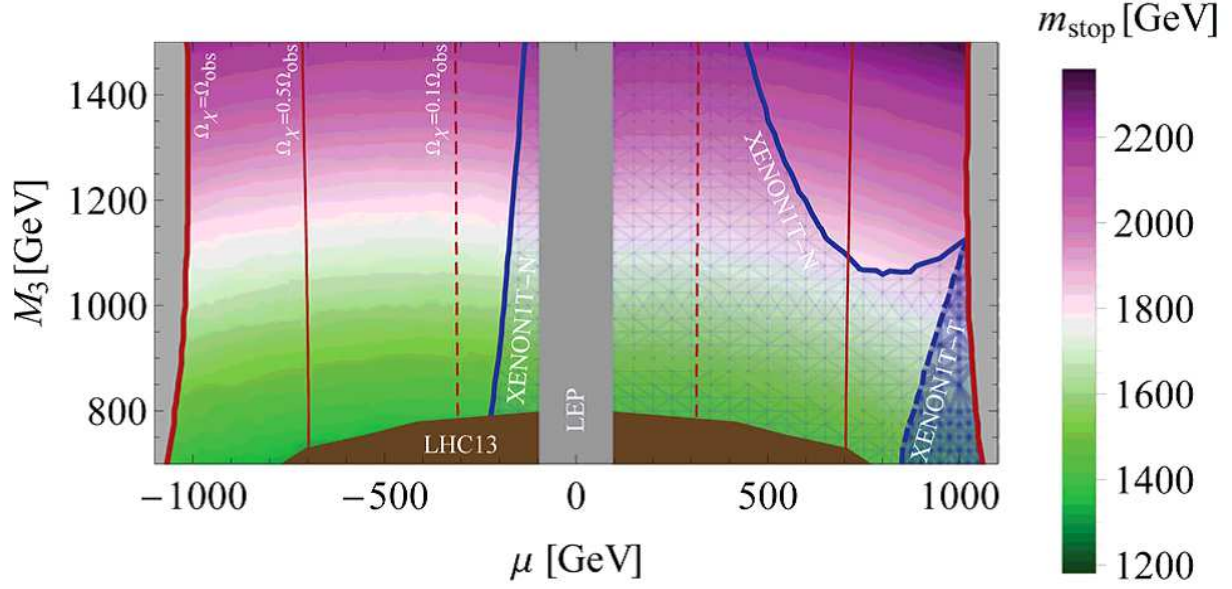


Figure 4: Values of the dark matter observables with $M_1 = 10$ TeV.

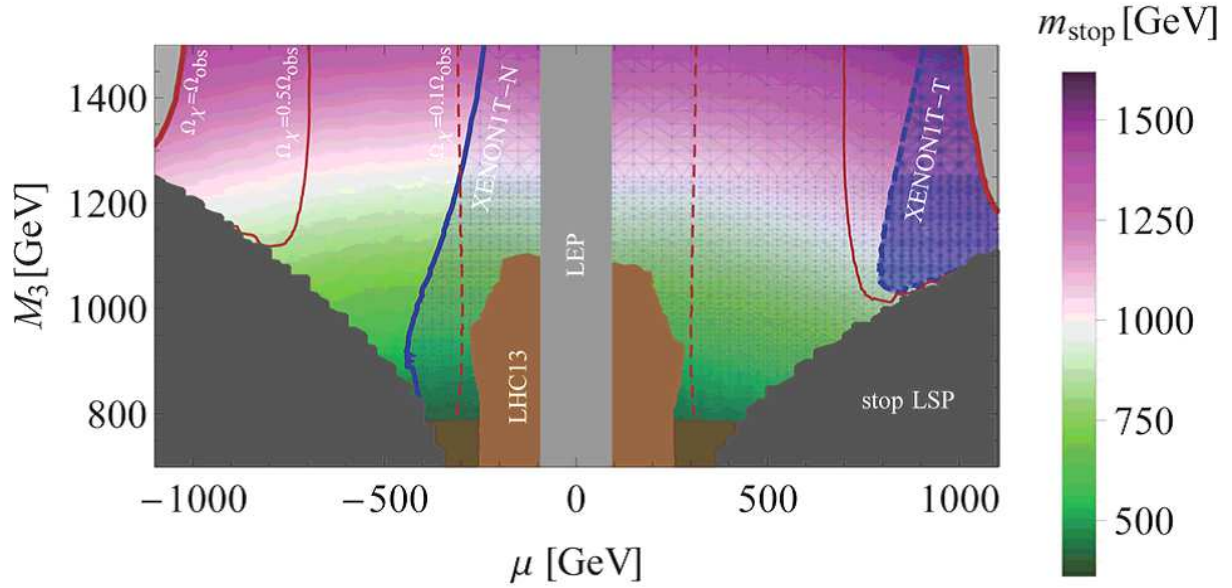


Figure 5: Values of the dark matter observables with $M_1 = 5.0$ TeV.

ment [61] in the blue band. This should be understood as the limits for the non-thermal scenario and the limit would be relaxed as the μ -parameter decreases in the thermal scenario. Such a suppression is, however, not so significant in this region, because the thermal relic density is enhanced due to the sizable fraction of bino to the lightest neutralino. The blue shaded

region covered by the solid blue lines (XENON1T-N) is the expected limit from the XENON1T experiment in the non-thermal case $\Omega_\chi = \Omega_{\text{obs}}$, while the dashed blue line (XENON1T-T) corresponds to the same limit in the thermal case, where the detection rate is suppressed due to the fewer neutralino relic density. Note that the cross section of the spin-independent direct detection is always larger than 0.25×10^{-10} pb in all figures in this paper. Then, we expect that the future experiments, the XENON1T [66] and the LZ [67], could cover our parameter region in the non-thermal scenario. On the other hand, the current limit from the spin-dependent cross section is fully covered by the spin-independent one.

The exclusion limit from the spin-independent cross section becomes stronger as the μ -parameter decreases in the non-thermal scenario. The reason is that the experimental limits for the cross section becomes tighter for lighter dark matter masses as long as the dark matter mass is heavier than about 40 GeV. On the other hand, this effect is erased by the smaller LSP density Ω_χ in the thermal scenario. The light bino mass region is easier to be excluded due to the large bino-higgsino mixing, especially the well-tempered region has already excluded by the current LUX limit as well known. The spin-independent cross section is significantly large for the positive μ -parameter compared with the case of the negative μ -parameter. This is because the cross section is proportional to $(1 + \text{sign}(\mu) \sin 2\beta)^2$ as can be read from Eq. (15).

Note that the exclusion limits on the μ - M_1 plane are severer than the ones derived in Ref. [68]. The difference comes from the fact that wino does not decouple completely in the NUGM scenario. In order to keep the μ -parameter smaller than 1 TeV, the wino mass at the unification scale has to be 3-4 times larger than the gluino mass. The higher wino-to-gluino ratio is required for the lower typical sparticle scale which is defined as the geometric mean of the top squark masses. In this case, (M_2, M_3) are about (4 TeV, 1.5 TeV) at the unification scale and it enhances the spin-independent cross section.

Figure 3 shows the allowed region for μ and M_1 at $M_3 = 1.0$ TeV. The different value of M_3 influences to the direct detection rate and the top squark mass. Top squark becomes the lightest SUSY particle in the dark gray region, and the top squark search at the LHC excludes the brown region. The LHC bounds are projected from the analysis in Ref. [9]. The bino mass has to be so large that top squark mass is larger than the higgsino mass.

The lighter gluino mass leads the lighter wino mass and the spin-independent cross section is enhanced by the wino-higgsino mixing. We see that the XENON1T experiment covers the whole region with $\mu > 0$ in the non-thermal scenario.

Figures 4 and 5 show the allowed region for μ and M_3 where M_1 is 5.0 TeV and 10.0 TeV at the unification scale, respectively. Other parameters are set to be the same as in Figures 2 and 3. The constraint from the gluino search at the LHC is also applied to these figures and it excludes the dark brown region. The gluino mass lower bound is around 800 GeV, so that there was no exclusion bounds in Figs. 2 and 3. We can see that experimental reaches from direct detections for the gluino mass can be much severer than those from the LHC experiment in the non-thermal scenario.

The wino-higgsino mixing is reduced as gluino becomes heavy. The mixing, however, is not vanishing in our model-dependent analysis. We see that the gaugino-higgsino mixing predicts

the spin-independent cross section larger than 2.5×10^{-11} pb everywhere in all of the four figures. Thus the parameter region is on the neutrino floor [85] and the region in our analysis would be fully covered by the future planned observations such as the XENON-nT, LZD, PandaX-4T and so on.

5 Conclusion

In this paper, we study the dark matter physics in the Non-Universal Gaugino Mass scenario. The NUGM scenario is one of the possible setups of the MSSM to achieve the 125 GeV Higgs boson mass and the μ -parameter below 1 TeV, that naturally explain the origin of the EW scale. Since one top squark is relatively light in our scenario, the authors in Refs. [7, 8] study the current status and the future prospect on the direct search for top squark and gluino at the LHC.

Although the higgsino mass is the most important from the naturalness point of view, higgsino can not be probed by the LHC due to their suitable mass difference ~ 2 GeV. On the other hand, the higgsino mass is critically important for dark matter physics and can be tested by the dark matter observations. The higgsino mass can not be larger than 1 TeV in order not to overclose the universe if we assume that there is no dilution effect after the LSP is frozen out.

Direct detections for dark matter are powerful tool to probe the neutralino sector of the MSSM. Even the bino and the wino masses are 3-4 TeV, the spin-independent cross section between higgsino and nucleon is in the observational reach. Therefore, the wider parameter space can be covered by the direct detection than the gluino search at the LHC, when the wino-to-gluino mass ratio is fixed to realize the small μ -parameter and the higgsino-like LSP dominates the relic density of dark matter.

If the neutralino density is determined by the standard thermal process, the direct detection is sensitive to the parameter region where the higgsino mass is around 1 TeV, while the top squark and the gluino searches at the LHC are generally sensitive to lighter higgsino. Thus the direct detection complement the direct search at the LHC.

The universal gaugino masses are clearly disfavored by the recent dark matter observations. The LSP is either bino or higgsino in this case, but the bino LSP easily overclose the universe. Even if the higgsino LSP is realized in some ways such as considered in Refs. [86, 87], light bino and wino are severely constrained by the direct detections. The direct detection constraints push up the gluino mass far above the experimental reach and such a heavy gluino indicates all other sparticles are also hopeless to be discovered except in some special cases. Thus the non-universal gaugino masses with relatively heavy bino and wino masses seems to be more interesting than the universal gaugino masses.

Acknowledgments

The work of J. K. was supported by Grant-in-Aid for Research Fellow of Japan Society for the Promotion of Science No. 16J04215.

References

- [1] S. P. Martin, In *Kane, G.L. (ed.): Perspectives on supersymmetry II* 1-153 [hep-ph/9709356].
- [2] D. J. H. Chung, L. L. Everett, G. L. Kane, S. F. King, J. D. Lykken and L. -T. Wang, Phys. Rept. **407**, 1 (2005) [hep-ph/0312378].
- [3] G. Jungman, M. Kamionkowski and K. Griest, Phys. Rept. **267** (1996) 195 [hep-ph/9506380].
- [4] G. Aad *et al.* [ATLAS and CMS Collaborations], Phys. Rev. Lett. **114** (2015) 191803 [arXiv:1503.07589 [hep-ex]].
- [5] H. Abe, T. Kobayashi and Y. Omura, Phys. Rev. D **76**, 015002 (2007) [hep-ph/0703044 [HEP-PH]].
- [6] H. Abe, J. Kawamura and H. Otsuka, PTEP **2013**, 013B02 (2013) [arXiv:1208.5328 [hep-ph]].
- [7] H. Abe, J. Kawamura and Y. Omura, JHEP **1508**, 089 (2015) [arXiv:1505.03729 [hep-ph]].
- [8] J. Kawamura and Y. Omura, Phys. Rev. D **93** (2016) no.5, 055019 [arXiv:1601.03484 [hep-ph]].
- [9] J.Kawamura, PhD thesis.
- [10] H. Baer, V. Barger, N. Nagata and M. Savoy, arXiv:1611.08511 [hep-ph]; H. Baer, V. Barger, N. Nagata and S. Michael, Phys. Rev. D **95**, no. 5, 055012 (2017).
- [11] H. Baer, V. Barger, J. S. Gainer, P. Huang, M. Savoy, D. Sengupta and X. Tata, arXiv:1612.00795 [hep-ph].
- [12] K. Choi, A. Falkowski, H. P. Nilles, M. Olechowski and S. Pokorski, JHEP **0411**, 076 (2004) [hep-th/0411066].
- [13] K. Choi, A. Falkowski, H. P. Nilles and M. Olechowski, Nucl. Phys. B **718**, 113 (2005) [hep-th/0503216].
- [14] K. Choi, K. S. Jeong and K. -i. Okumura, JHEP **0509**, 039 (2005) [hep-ph/0504037].

- [15] A. Brignole, L. E. Ibanez, C. Munoz and C. Scheich, *Z. Phys. C* **74**, 157 (1997) [hep-ph/9508258].
- [16] A. Brignole, L. E. Ibanez and C. Munoz, In *Kane, G.L. (ed.): Perspectives on supersymmetry II* 244-268 [hep-ph/9707209].
- [17] L. Randall and R. Sundrum, *Nucl. Phys. B* **557** (1999) 79 [hep-th/9810155];
- [18] G. F. Giudice, M. A. Luty, H. Murayama and R. Rattazzi, *JHEP* **9812** (1998) 027 [hep-ph/9810442].
- [19] K. Choi, K. S. Jeong, T. Kobayashi and K. -i. Okumura, *Phys. Lett. B* **633**, 355 (2006) [hep-ph/0508029]; K. Choi, K. S. Jeong, T. Kobayashi and K. -i. Okumura, *Phys. Rev. D* **75**, 095012 (2007) [hep-ph/0612258].
- [20] R. Kitano and Y. Nomura, *Phys. Lett. B* **631** (2005) 58 [hep-ph/0509039].
- [21] K. Choi, K. Y. Lee, Y. Shimizu, Y. G. Kim and K. -i. Okumura, *JCAP* **0612**, 017 (2006) [hep-ph/0609132].
- [22] W. S. Cho, Y. G. Kim, K. Y. Lee, C. B. Park and Y. Shimizu, *JHEP* **0704**, 054 (2007) [hep-ph/0703163 [HEP-PH]].
- [23] M. Nagai and K. Nakayama, *Phys. Rev. D* **76**, 123501 (2007) [arXiv:0709.3918 [hep-ph]].
- [24] S. Nakamura, K. -i. Okumura and M. Yamaguchi, *Phys. Rev. D* **77**, 115027 (2008) [arXiv:0803.3725 [hep-ph]].
- [25] K. Choi, K. S. Jeong, S. Nakamura, K. -I. Okumura and M. Yamaguchi, *JHEP* **0904**, 107 (2009) [arXiv:0901.0052 [hep-ph]].
- [26] M. Holmes and B. D. Nelson, *JCAP* **0907**, 019 (2009) [arXiv:0905.0674 [hep-ph]].
- [27] B. Altunkaynak, B. D. Nelson, L. L. Everett, I. -W. Kim and Y. Rao, *JHEP* **1005**, 054 (2010) [arXiv:1001.5261 [hep-ph]].
- [28] L. L. Everett, I. -W. Kim, P. Ouyang and K. M. Zurek, *JHEP* **0808**, 102 (2008) [arXiv:0806.2330 [hep-ph]].
- [29] L. L. Everett, I. -W. Kim, P. Ouyang and K. M. Zurek, *Phys. Rev. Lett.* **101**, 101803 (2008) [arXiv:0804.0592 [hep-ph]].
- [30] M. Asano and T. Higaki, *Phys. Rev. D* **86**, 035020 (2012) [arXiv:1204.0508 [hep-ph]].
- [31] T. Kobayashi, H. Makino, K. i. Okumura, T. Shimomura and T. Takahashi, *JHEP* **1301**, 081 (2013) [arXiv:1204.3561 [hep-ph]].

- [32] H. Abe and J. Kawamura, JHEP **1407** (2014) 077 [arXiv:1405.0779 [hep-ph]].
- [33] K. Hagimoto, T. Kobayashi, H. Makino, K. i. Okumura and T. Shimomura, JHEP **1602**, 089 (2016) [arXiv:1509.05327 [hep-ph]].
- [34] L. L. Everett, T. Garon, B. L. Kaufman and B. D. Nelson, Phys. Rev. D **93**, no. 5, 055031 (2016) [arXiv:1510.05692 [hep-ph]].
- [35] V. Barger, L. L. Everett and T. S. Garon, Phys. Rev. D **93**, no. 7, 075024 (2016) [arXiv:1512.05011 [hep-ph]].
- [36] H. Baer, V. Barger, H. Serce and X. Tata, Phys. Rev. D **94**, no. 11, 115017 (2016) [arXiv:1610.06205 [hep-ph]].
- [37] J. E. Yunkin and S. P. Martin, Phys. Rev. D **85**, 055028 (2012) [arXiv:1201.2989 [hep-ph]].
- [38] R. Blumenhagen, B. Kors, D. Lust and S. Stieberger, Phys. Rept. **445**, 1 (2007) [hep-th/0610327].
- [39] R. Barbieri and G. F. Giudice, Nucl. Phys. B **306** (1988) 63.
- [40] J. Kawamura and Y. Omura, in preparation.
- [41] M. Ibe, T. Moroi and T. T. Yanagida, Phys. Lett. B **644**, 355 (2007) [hep-ph/0610277].
- [42] R. Mahbubani, P. Schwaller and J. Zurita, arXiv:1703.05327 [hep-ph].
- [43] H. Fukuda, N. Nagata, H. Otono and S. Shirai, arXiv:1703.09675 [hep-ph].
- [44] The ATLAS collaboration, ATLAS-CONF-2015-066.
- [45] The ATLAS collaboration, ATLAS-CONF-2016-077
- [46] The ATLAS collaboration, ATLAS-CONF-2016-052.
- [47] The ATLAS collaboration, ATLAS-CONF-2016-078
- [48] M. Cirelli, N. Fornengo and A. Strumia, Nucl. Phys. B **753**, 178 (2006) [hep-ph/0512090].
- [49] M. Cirelli, A. Strumia and M. Tamburini, Nucl. Phys. B **787**, 152 (2007) [arXiv:0706.4071 [hep-ph]].
- [50] N. Arkani-Hamed, A. Delgado and G. F. Giudice, Nucl. Phys. B **741**, 108 (2006) [hep-ph/0601041].
- [51] K. Hamaguchi and K. Ishikawa, Phys. Rev. D **93** (2016) no.5, 055009 [arXiv:1510.05378 [hep-ph]].

- [52] P. A. R. Ade *et al.* [Planck Collaboration], *Astron. Astrophys.* **594**, A13 (2016) [arXiv:1502.01589 [astro-ph.CO]].
- [53] K. Kohri, M. Yamaguchi and J. Yokoyama, *Phys. Rev. D* **72**, 083510 (2005) [hep-ph/0502211].
- [54] H. Baer, A. Lessa and W. Sreethawong, *JCAP* **1201**, 036 (2012) [arXiv:1110.2491 [hep-ph]].
- [55] H. Baer, K. Y. Choi, J. E. Kim and L. Roszkowski, *Phys. Rept.* **555**, 1 (2015) [arXiv:1407.0017 [hep-ph]].
- [56] R. Allahverdi, M. Cicoli, B. Dutta and K. Sinha, *Phys. Rev. D* **88**, no. 9, 095015 (2013) [arXiv:1307.5086 [hep-ph]].
- [57] M. Garny, A. Ibarra, M. Pato and S. Vogl, *Phys. Rev. D* **87** (2013) no.5, 056002 [arXiv:1211.4573 [hep-ph]].
- [58] E. Aprile *et al.* [XENON100 Collaboration], *Phys. Rev. Lett.* **109**, 181301 (2012) [arXiv:1207.5988 [astro-ph.CO]].
- [59] E. Aprile *et al.* [XENON100 Collaboration], *Phys. Rev. Lett.* **111**, no. 2, 021301 (2013) [arXiv:1301.6620 [astro-ph.CO]].
- [60] D. S. Akerib *et al.* [LUX Collaboration], *Phys. Rev. Lett.* **116**, no. 16, 161301 (2016) [arXiv:1512.03506 [astro-ph.CO]].
- [61] D. S. Akerib *et al.*, arXiv:1608.07648 [astro-ph.CO].
- [62] A. Tan *et al.* [PandaX-II Collaboration], *Phys. Rev. Lett.* **117**, no. 12, 121303 (2016) [arXiv:1607.07400 [hep-ex]].
- [63] C. Fu *et al.* [PandaX-II Collaboration], *Phys. Rev. Lett.* **118**, no. 7, 071301 (2017) [arXiv:1611.06553 [hep-ex]].
- [64] C. Amole *et al.* [PICO Collaboration], *Phys. Rev. D* **93**, no. 5, 052014 (2016) [arXiv:1510.07754 [hep-ex]].
- [65] C. Amole *et al.* [PICO Collaboration], *Phys. Rev. D* **93**, no. 6, 061101 (2016) [arXiv:1601.03729 [astro-ph.CO]].
- [66] E. Aprile *et al.* [XENON Collaboration], *JCAP* **1604**, no. 04, 027 (2016) [arXiv:1512.07501 [physics.ins-det]].
- [67] D. S. Akerib *et al.* [LZ Collaboration], arXiv:1509.02910 [physics.ins-det].

- [68] C. Cheung, L. J. Hall, D. Pinner and J. T. Ruderman, JHEP **1305** (2013) 100 [arXiv:1211.4873 [hep-ph]].
- [69] G. Belanger, F. Boudjema, A. Pukhov and A. Semenov, Comput. Phys. Commun. **185**, 960 (2014) [arXiv:1305.0237 [hep-ph]]; G. Belanger, F. Boudjema, A. Pukhov and A. Semenov, Comput. Phys. Commun. **174**, 577 (2006) [hep-ph/0405253]; G. Belanger, F. Boudjema, A. Pukhov and A. Semenov, Comput. Phys. Commun. **149**, 103 (2002) [hep-ph/0112278].
- [70] G. Belanger, F. Boudjema, A. Pukhov and A. Semenov, Comput. Phys. Commun. **192**, 322 (2015) [arXiv:1407.6129 [hep-ph]].
- [71] G. Belanger, F. Boudjema, A. Pukhov and A. Semenov, Comput. Phys. Commun. **180** (2009) 747 [arXiv:0803.2360 [hep-ph]].
- [72] M. Drees and M. Nojiri, Phys. Rev. D **48**, 3483 (1993) [hep-ph/9307208].
- [73] J. Hisano, K. Ishiwata, N. Nagata and T. Takesako, JHEP **1107**, 005 (2011) [arXiv:1104.0228 [hep-ph]].
- [74] M. G. Aartsen *et al.* [IceCube Collaboration], Eur. Phys. J. C **77**, no. 3, 146 (2017) [arXiv:1612.05949 [astro-ph.HE]].
- [75] M. Ackermann *et al.* [Fermi-LAT Collaboration], Phys. Rev. Lett. **115**, no. 23, 231301 (2015) [arXiv:1503.02641 [astro-ph.HE]].
- [76] M. Aguilar *et al.* [AMS Collaboration], Phys. Rev. Lett. **117**, no. 9, 091103 (2016).
- [77] A. Cuoco, M. Krämer and M. Korsmeier, arXiv:1610.03071 [astro-ph.HE].
- [78] M. Y. Cui, Q. Yuan, Y. L. S. Tsai and Y. Z. Fan, arXiv:1610.03840 [astro-ph.HE].
- [79] G. A. Gomez-Vargas *et al.*, JCAP **1310**, 029 (2013) [arXiv:1308.3515 [astro-ph.HE]].
- [80] J. Carr *et al.* [CTA Collaboration], PoS ICRC **2015**, 1203 (2016) [arXiv:1508.06128 [astro-ph.HE]].
- [81] L. Aparicio, M. Cicoli, B. Dutta, F. Muia and F. Quevedo, JHEP **1611**, 038 (2016) [arXiv:1607.00004 [hep-ph]].
- [82] B. C. Allanach, Comput. Phys. Commun. **143**, 305 (2002) [hep-ph/0104145].
- [83] A. Djouadi, M. M. Muhlleitner and M. Spira, Acta Phys. Polon. B **38**, 635 (2007) [hep-ph/0609292]; M. Muhlleitner, A. Djouadi and Y. Mambrini, Comput. Phys. Commun. **168**, 46 (2005) [hep-ph/0311167]; A. Djouadi, J. Kalinowski and M. Spira, Comput. Phys. Commun. **108**, 56 (1998) [hep-ph/9704448].

- [84] K. Jakobs, hep-ex/0107084.
- [85] J. Billard, L. Strigari and E. Figueroa-Feliciano, Phys. Rev. D **89**, no. 2, 023524 (2014) [arXiv:1307.5458 [hep-ph]].
- [86] J. L. Feng and D. Sanford, Phys. Rev. D **86**, 055015 (2012) [arXiv:1205.2372 [hep-ph]].
- [87] H. Baer, V. Barger, P. Huang, A. Mustafayev and X. Tata, Phys. Rev. Lett. **109**, 161802 (2012) [arXiv:1207.3343 [hep-ph]].